EUROPEAN COMMISSION

Community research

Long-term Performance of Engineered Barrier Systems

Long-term Performance of Engineered Barrier Systems PEBS

Engineered Barrier Emplacement Experiment in Opalinus Clay: "EB" Experiment

Horizontal borehole results (geophysics, hydro test, laboratory tests)

(DELIVERABLE-N°: D2.1-1)

Contract (grant agreement) number: FP7 249681

Authors:

Kristof Schuster[1], Markus Furche[1], Manuel Velasco[2], Irina Gaus[3], Thomas Trick[4], José Luis García-Siñeriz[5], María Rey[5], Friedhelm Schulte[1], Silvio Sanchez Herrero[1], Torsten Tietz[1], Juan Carlos Mayor[6]

[1] BGR, Germany, [2] Golder, Spain, [3] Nagra, Switzerland, [4] Solexperts, Switzerland, [5] Aitemin, Spain, [6] Enresa, Spain

Date of issue of this report: 11/04/2014

Start date of project: 01/03/10 Duration : 48 Months

Project co-funded by the European Commission under the Seventh Euratom Framework Programme for Nuclear Research &Training Activities (2007-2011)		
Dissemination Level		
PU	Public	**PU**
RE	Restricted to a group specified by the partners of the [acronym] project	
CO	Confidential, only for partners of the [acronym] project	

EURATOM

Table of Contents

List of Figures

List of Tables

1 Introduction

The Engineered Barrier Emplacement Experiment in Opalinus Clay (EB) is a long running experiment which started in 2000 and was incorporated in 2010 into the PEBS Project (Long-term performance of Engineered Barrier Systems) and was assumed to be finished beginning 2013 with a full dismantling. In the run-up to the dismantling activities, planned for autumn and winter 2012, in August 2011 the drilling of two pilot boreholes was planned. This task aimed at the characterisation of the emplaced bentonite after its saturation with the help of analyzing fresh sample material in the laboratory, performing geophysical borehole measurements in one of the boreholes and performing hydro tests in the second borehole. The chosen geophysical methods were ultrasonic and geoelectrical high resolution borehole methods.

The history and some of the background information of both experiments was compiled already in the PEBS Deliverable D2.1-4 by Palacios et al. (2013, sections 1.1 and 1.2.1) and is resumed here and extended with the information concerning the geophysical and geotechnical activities which were at the responsibility of BGR.

1.1 The EB project

The Engineered Barrier Emplacement Experiment in Opalinus Clay (EB Experiment) aimed at demonstrating a new concept for the construction of HLW repositories in horizontal drifts, in competent clay formations. The principle of the new construction method was based on the combined use of a lower bed made of compacted bentonite blocks, and an upper buffer made of granular bentonite material (GBM). The project consisted on a real scale isothermal simulation of this construction method in the Opalinus Clay formation at the Mont Terri underground laboratory in Switzerland. A steel dummy canister, with the same dimensions and weight as the Spanish reference canister, was placed on top of a bed of bentonite blocks, and then the upper part of the drift was buffered with the GBM made of bentonite pellets (Figure 1). The drift was sealed with a concrete plug having a concrete retaining wall between the plug and the GBM. Since the end of the test installation the evolution of the different hydro-mechanical parameters were monitored, both in the barrier and the rock (especially in the Excavation Disturbed Zone (EDZ)). Relative humidity and temperature in the rock and in the bentonite buffer, rock and canister displacement, pore pressure and total pressure were registered by means of different types of sensors. Due to the short amount of

free water available in this formation, an artificial hydration system was installed to accelerate the hydration process in the bentonite.

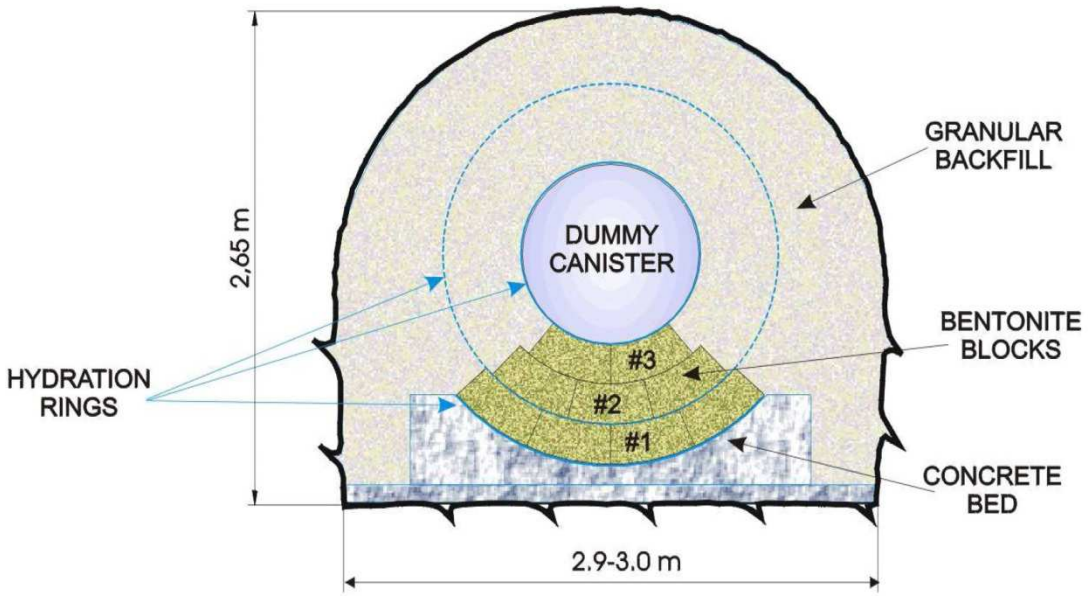

Figure 1: EB experimental layout

The basic objectives of the project were the following:

- Definition of backfill material (composition, grain size distribution ...). Demonstration of the manufacturing process at semi-industrial scale.
- Characterization of the hydro-mechanical properties of the backfill material.
- Design and demonstration of the emplacement and backfilling technique.
- Quality Assessment of the clay barrier in terms of the achieved geomechanical parameters (homogeneity, dry density, voids distribution ...) after emplacement.
- Characterization of the EDZ in the Opalinus Clay, and determination of its influence in the overall performance of the system.
- Investigation of the evolution of the hydro-mechanical parameters in the clay barrier and the EDZ as a function of the progress of the hydration process.
- Development of a hydro-mechanical model of the complete system adjusted and calibrated with the data resulting from the experiment.

After 10.5 years of operation, the experiment has been dismantled between the 19th of October 2012 and the 1st of February 2013. The aim of this document is to describe the

design, results and conclusions of distinct time steps of the geoelectrical monitoring of the dismantling operation.

1.2 Background

1.2.1 Funding

The first phase of the EB experiment - years 2000 to 2003 - devoted to the test design, installation and start-up of the operation, was co-financed by the European Commission (contract nº FIKW-CT-2000-00017), under the framework of the research and training programme (Euratom) in the field of nuclear energy, and ENRESA (Spain). Besides ENRESA, BRG (Germany) and NAGRA (Switzerland) were the principal contractors and AITEMIN (Spain) and CIMNE (Spain) the assistant contractors.

Between 2003 and 2009 the project operation continued under the support of the Mont Terri Consortium, project 32.015: EB, phases 10 to 14.

From 2010, the experiment is part of the PEBS project, Work Package 2 Experimentation. The PEBS project is one of the “Small and Medium Projects” forming part of the FP7 Euratom programme. It is a multinational European research project that investigates processes affecting the engineered barrier performance of geological repositories for high-level waste disposal. The PEBS consortium consists of 17 leading nuclear research organizations, radioactive waste management agencies/implementing organizations, universities and companies.

1.2.2 Experimental sequence

After the preparation of the design document (Aitemin, 2001) and the components procurement, the installation of the experiment was carried out in several steps. The instrumentation was installed from November 2001 to February 2002: in-rock pore pressure sensors, rock displacement sensors and some rock relative humidity sensors, canister displacement sensors, relative humidity sensors in bentonite and total pressure cells. The artificial hydration system was installed in March 2002. The installation of the experiment was finished in April 2002, including the retaining wall, the concrete plug and the data acquisition system.

The artificial hydration of the bentonite started in May 2002 and ended in June 2007. There was an initial hydration phase with a significant amount of water injected (6,700 litres in two days) that was stopped after several water stains appeared on the wall. After that, the hydration was restarted and from September 2002 to June 2007, there were different hydration phases with continuous water injection. The detailed record of effective water inflow for bentonite hydration is included in report SDR EB N19 (Aitemin, 2007).

After the end of the hydration phase, the monitoring of the experiment continued in order to follow the evolution of the bentonite.

The Engineered Barrier Emplacement Experiment is described in detail in the “EB Experiment Test Plan”, Project Deliverable 1, EC contract FIKW-CT2000-00017 (Aitemin, 2001), which includes the preliminary design, the emplacement and the operation.

BGR was in charge of performing at different stages of the EB experiment several geophysical and geotechnical oriented measurements for the characterization of the EBS, partly with subcontractors (TU Berlin, GMuG and Solexperts). For the initial characterization of the EB niche, immediately after the excavation, ultrasonic / seismic and geoelectrical measurements were performed in boreholes as well as along profiles (June 2001 – November 2001). After the closure of the niche (end of April 2002) and the start of the hydration phase (beginning of May 2002) a seismic long-term monitoring started (April 2002 – November 2003), including an acoustic emission experiment (April 2002 – April 2003). In November 2002 and one year later, in November 2003, geoelectrical measurements in the backfilled niche were conducted. The hydraulic characterization was executed in five stages between October 2001 and October 2003. These activities are documented in Schuster et al., 2004B. In August 2011, more than nine years after the closure, BGR drilled two horizontal pilot boreholes for the characterization of the bentonite. Geophysical measurements (geoelectrical and ultrasonic), sampling of bentonite at different depths and preparations for a hydro test were done in August 2011 (this report). In July 2012 the seismic long-term monitoring was resumed in order to monitor the expected changes in rock and bentonite parameters during the dismantling process in winter 2012 (Schuster, 2014). This monitoring is ongoing. For the same reason a geoelectrical circular profile was reactivated and was used for daily measurements between September 2012 and May 2013 (Furche and Schuster, 2014).

2 Drilling of two pilot boreholes

The main task of the work performed by several participants in this work package was the drilling of two pilot boreholes through the concrete plug into the saturated backfill material. The first borehole (BEB-PB1) was used step-by-step during the drilling and / or afterwards for sampling of compacted bentonite material (see Chap. 3), for high resolution geoelectrical borehole measurements (see Chap. 4), ultrasonic borehole measurements (see Chap. 5) and the second borehole (BEB-PB2) was planned for a hydro test (see Chap. 6). The objectives and the design of the boreholes were described in a specific document (Aitemin, 2011). The planned locations of both boreholes are shown in Figure 2, whereas the longitudinal section of the EB niche is presented in Figure 3. For the location of the boreholes the distribution of the inner elements (canister, sensors, hydration pipes) and the outer elements (instrumentation cable boxes, concrete plug reinforcement bars) had to be taken into account.

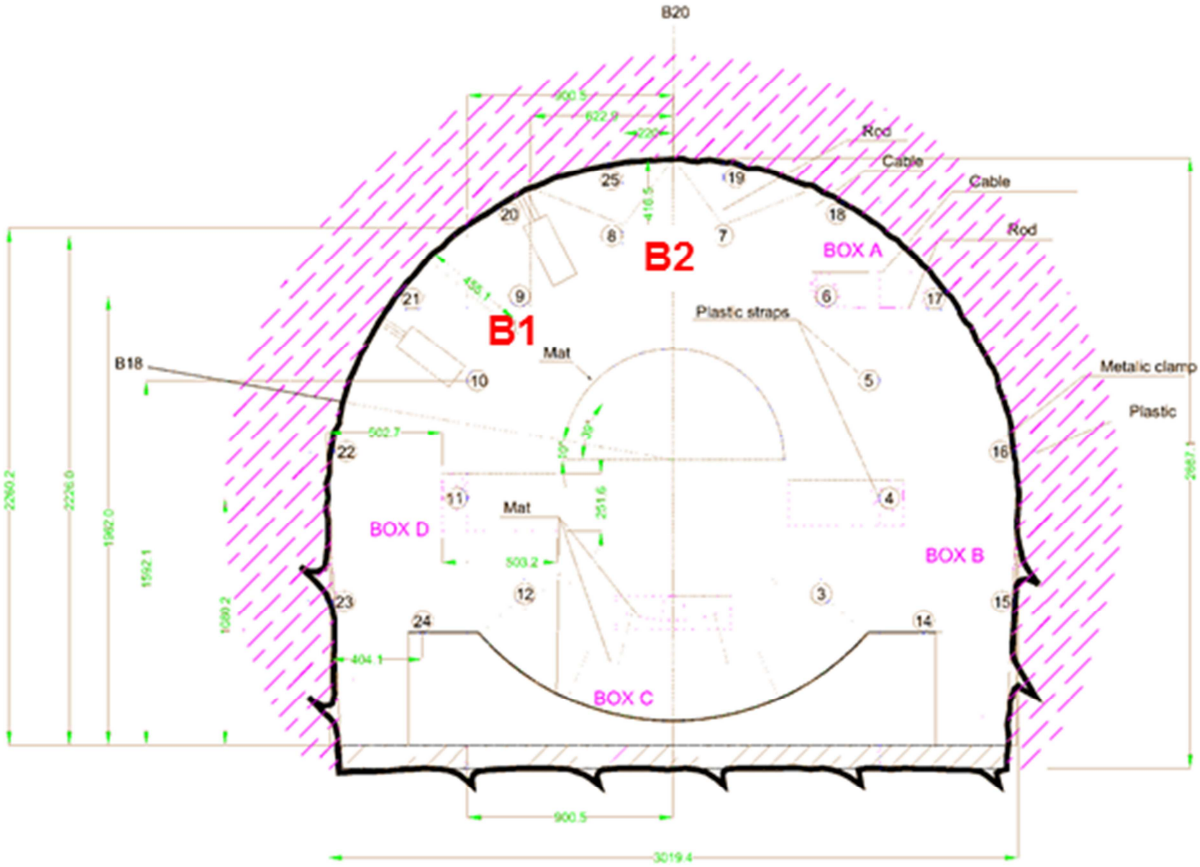

Figure 2: Locations of borehole mouths of boreholes B1 (BEB-PB1) and B2 (BEB-PB2)

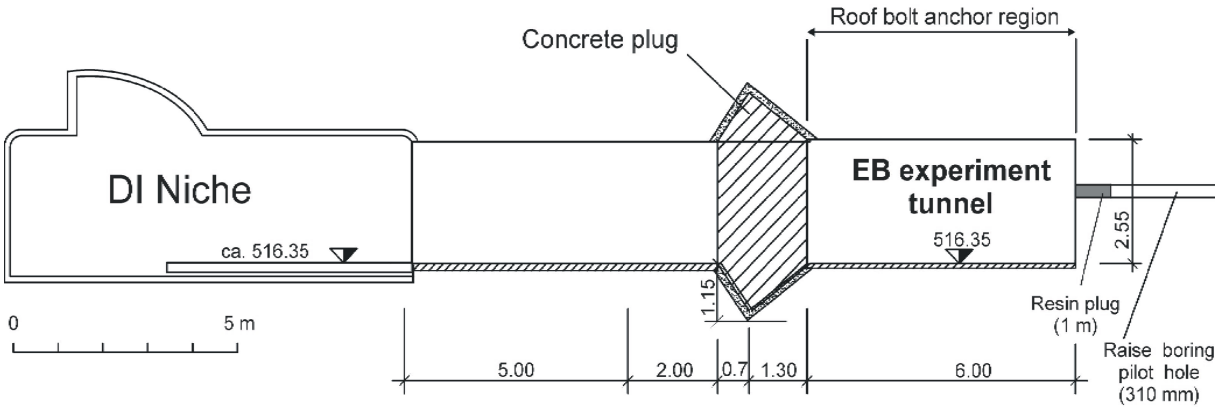

Figure 3: Longitudinal section of the EB niche

The details of all on-site activities performed in the task “pilot borehole” are compiled in the following Table 1.

Table 1: On-site activities performed within the pilot borehole task (KM: core meter). Geophysical measurements marked in colour.

Date	Time	Activity
		Drilling equipment
		Hilti drilling engine DD-750 Hy
		Hilti drilling aggregate D-LP 15
		BEB-PB 1
16.08.11		Installation of drilling equipment and site preparation
17.08.11	08:15 - 09:15	KM 1: 0m – 0.90m, concrete, outer Ø112mm, inner Ø 104mm
18.08.11	09:30 - 11:05	KM 2: 0.90m – 1.90m, concrete
23.08.11	08:40	KM 3: 1.90m – 2.22m, Ø 86mm, concrete
		2.22m – 2.28m, bentonite
		KM 4: 2.2m – 2.43m, Ø 86mm
		KM 5: 2.52m – 2.76m, Ø 86mm
		KM 6: 2.76m – 3.20 m, Ø 86mm
	15:40	Geoelektric: Position: 3.0m, 0°
	17:20	Geoelektric: Position: 3.0m, 180°
	18:00	Ultrasonic measurements: Position: 2.95m, 0°
	18:30	KM 7: 3.20m – 3.35m, Ø 86mm
	19:30	KM 8: 2.20m – 3.79m, Overcoring Ø 101mm
24.08.11	08:30	KM 9: 3.79m – 4.0m, Ø 86mm
		KM10: 3.79m – 4.01m, Overcoring Ø 101mm
	09:20	KM11: 4.01m – 4.24m, Ø 101mm / end of drilling

	09:35 - 10:00	Geoelektric: Position: 3,55m, 180°, 0°
	16:20 - 17:30	Geoelektric: Position: 2.95m_180°, 3,55m_180°, 4,05m_0°, 180°
	10:30	Ultrasonic measurements: Position 2.40m - 3,58m_ 0°
	15:40	Ultrasonic measurements: Position 2.40m – 4.10m_0°
		BEB-PB 2
25.08.11	08:30	KM1: Ø112mm, 0,0m - 1,0m concrete
		KM2: Ø112mm, 1,0m - 1,25m concrete
	12:00	KM3: Ø112mm, 1,25m-2,15m concrete
	13:30	KM4: Ø90mm, 2,15m - 2,60m bentonite
		KM5: Ø90mm, 2,60m - 2,84m
		KM6: Ø90mm, 2,84m - 3,08m
		KM7: Ø90mm, 3,08m - 3,61m
	17:00	KM8: Ø90mm, 3,61m - 3,86m
26.08.11	08:30	KM9: Ø90mm, 3,86m - 4,12m
	11:30	KM10: Ø101mm, 2,22m - 4,19m overcoring
	11:30 - 13:00	Installation of casing for hydro test equipment
	13:30 - 14:30	Rasin injection of annular space between casing and borehole wall within the concrete plug section
	14:30 - 17:00	Set of double packer system

2.1 Drilling technique

As there was no previous experiences concerning drilling and controlled sampling in consolidated bentonites a technical discussion was held before involving all the partners of the experiment in order to discuss and finally to choose the best strategy for the drilling and especially for the sampling (Technical Discussion Meeting, February 17, 2011, Saint Ursanne). As an outcome of this discussion both boreholes with diameters ranging from 112 mm to 86 mm, should be drilled with a well-established Hilti drilling machine which was operated by BGR staff. The photographs presented as Figures 4 and 5 give an impression of the on-site work, whereas Figures 6 and 7 show details of the drilling equipment and the process.

Figure 4: Drilling operation in the EB niche in borehole BEB-PB2

Figure 5: Cleaning of a drilling rod, clotted with bentonite

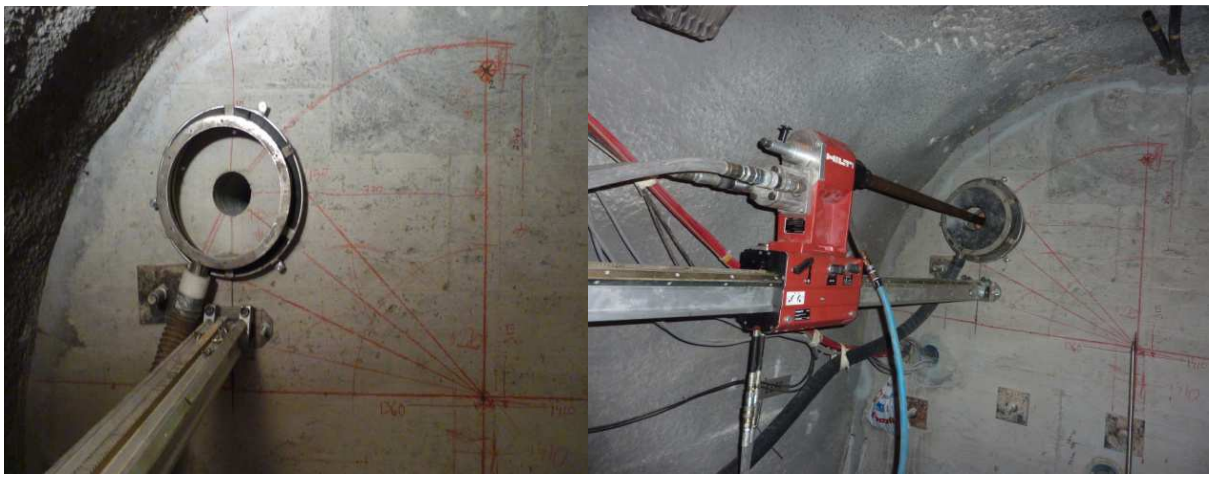

Figure 6: Borehole mouth of borehole BEB-PB1 (left) and details of the drilling equipment in front of the concrete plug (right)

Figure 7: Sampler filled with bentonite

Two boreholes were drilled through the 2.2 m thick concrete plug (see Figure 4) and approximately 2 m further into the backfilled niche.

- Borehole 1 (BEB-PB1) was set at about 10 o'clock on the left hand side of the niche and aimed to run close to the seismic array which was installed in spring 2002. The drilling work for borehole 1 was combined with a stepwise sampling of bentonite specimen and geophysical measurements at several depths.
- Borehole 2 (BEB-PB2) was set in a central position at about 12 o'clock. It was drilled after the first one and immediately instrumented with a hydraulic double packer system provided by Solexperts.

The proposed and partly applied drilling technique for both boreholes is explained in Figures 8 to 12 step by step. In case of drilling and installing the double packer system in borehole 2 some steps were ignored and others are extended, but the principal work flow was similar.

In order to stabilize parts of the drilled borehole barrels with different inner and outer diameters were used. The idea was to provide a type of telescoping system that guaranteed a save retrieval of the temporally used tools, e. g. geophysical borehole tools or the sampling tool. The principal is compiled in Figure 8.

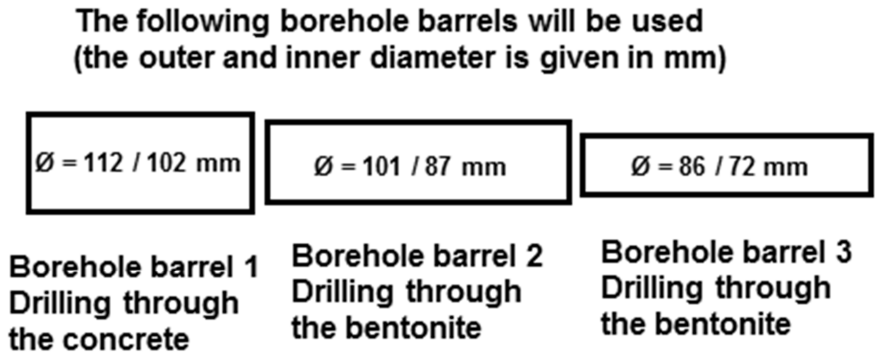

Figure 8: Drilling with a telescopic system consisting of barrels with different diameters.

After crossing the 2.2 m thick concrete plug the following work sequence was performed:

1. Take samples by pushing a special sampling tool with the help of the drilling machine into the bentonite
2. Continue drilling until 1 m with a diameter of 86 mm
3. Perform geophysical borehole measurements
4. Drill this part with a diameter of 112 mm
5. Emplace a liner for the stabilization of the first section (0 – 1 m)
6. Continue with the sampling between 1 m and 2 m, and so on.

The complete sequence of all steps is presented in a graphical visualisation in the following Figures 9 to 12.

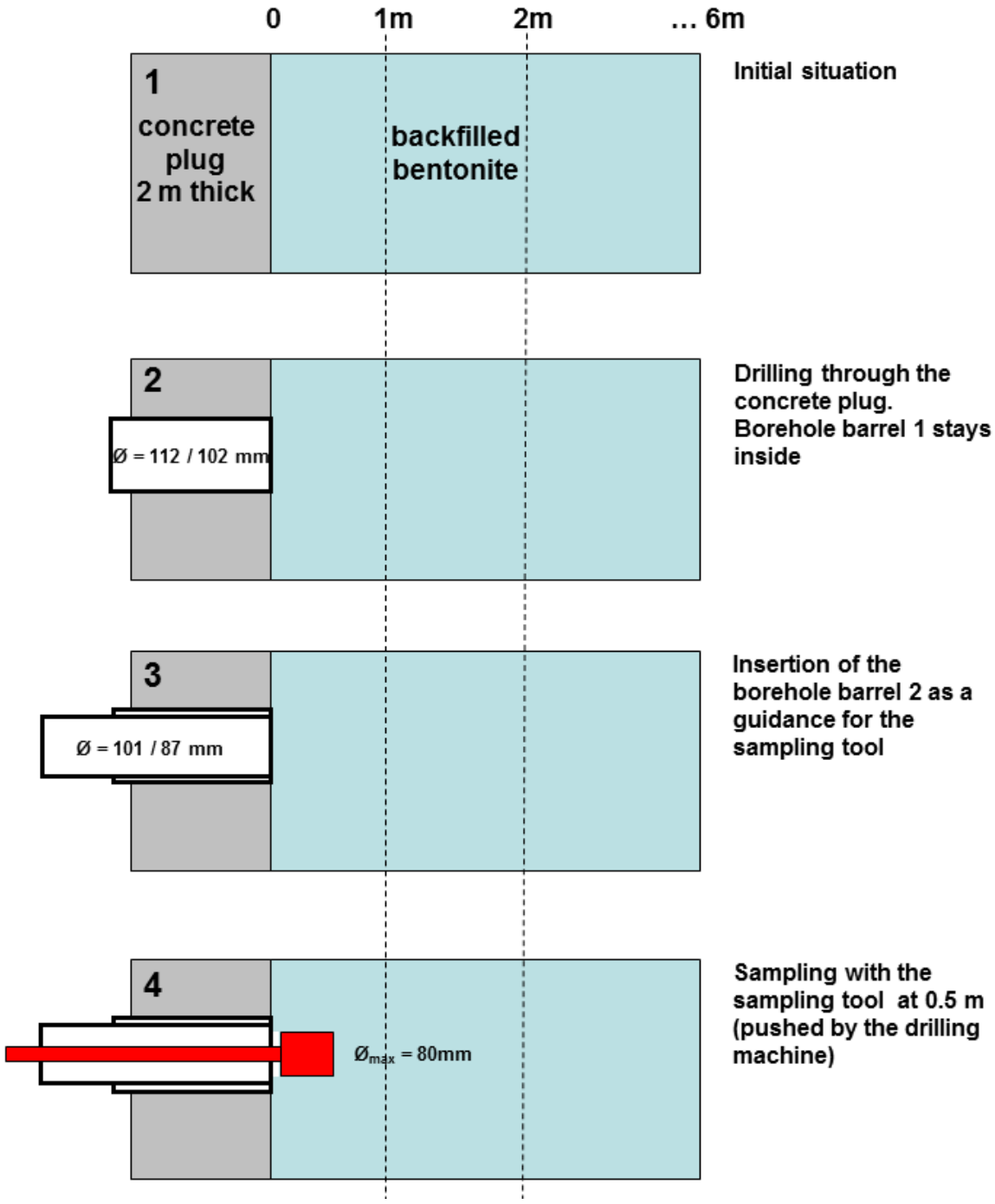

Figure 9: Part 1 - Graphical visualization of the drilling, sampling and geophysical measurement sequence applied in the pilot boreholes.

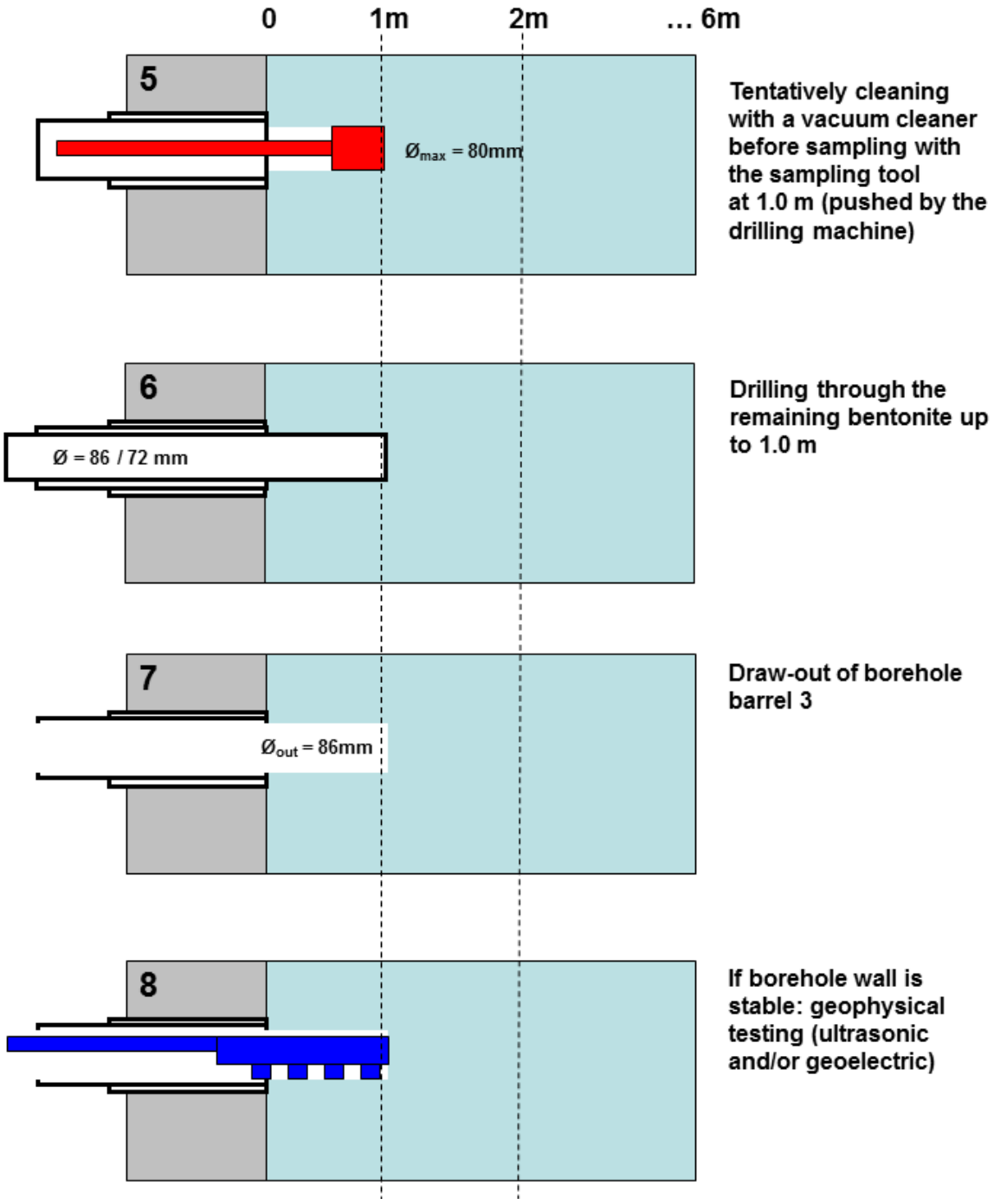

Figure 10: Part 2 - Graphical visualization of the drilling, sampling and geophysical measurement sequence applied in the pilot boreholes.

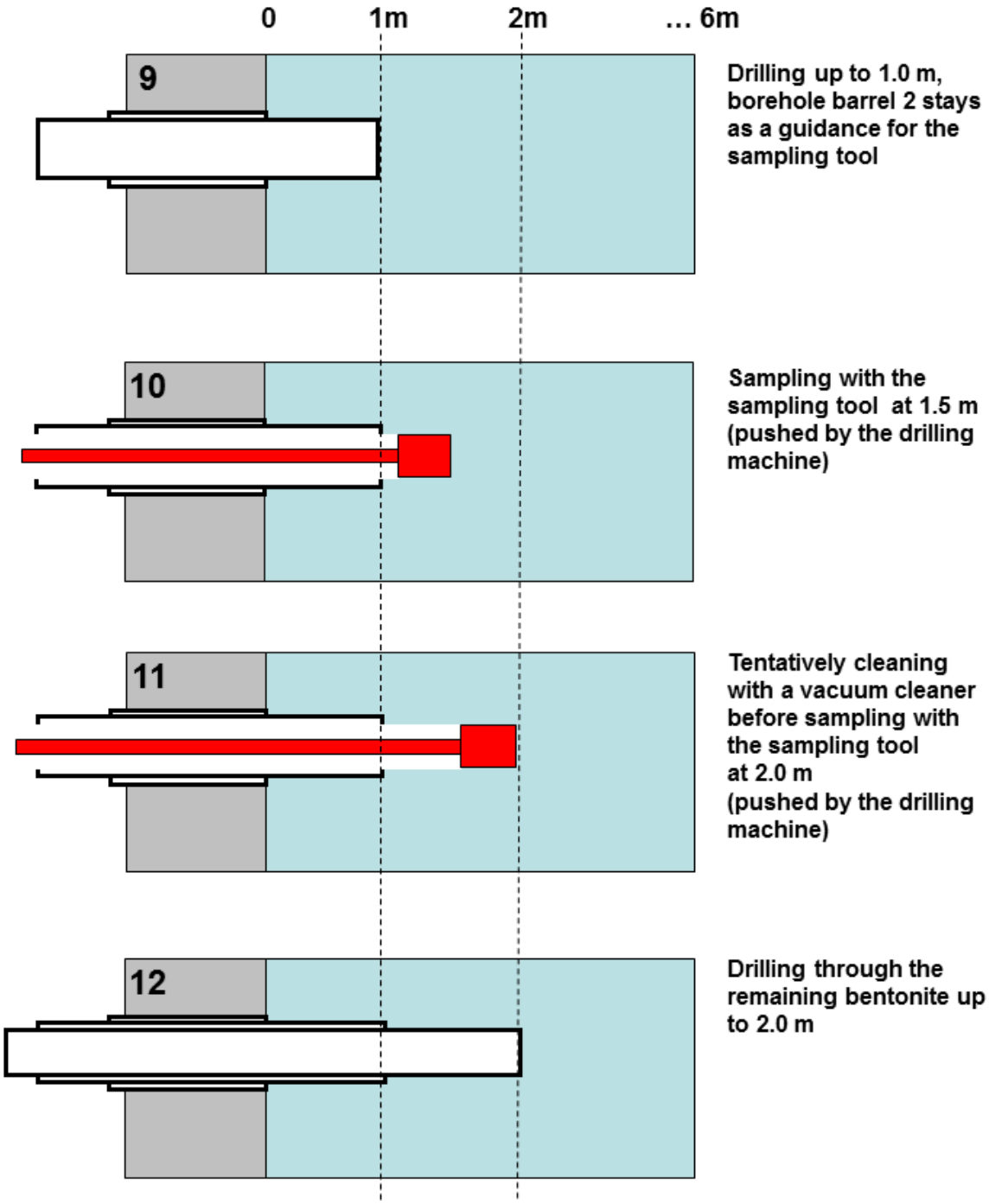

Figure 11: Part 3 - Graphical visualization of the drilling, sampling and geophysical measurement sequence applied in the pilot boreholes.

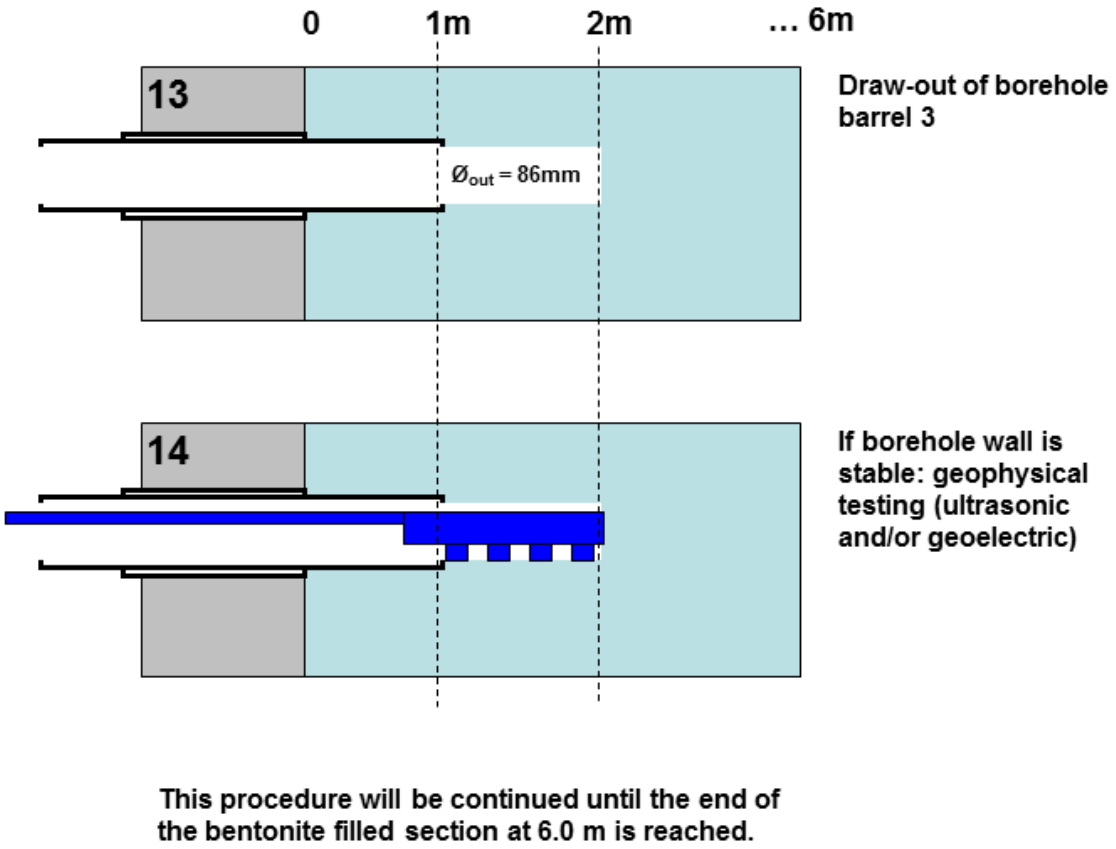

Figure 12: Part 4 - Graphical visualization of the drilling, sampling and geophysical measurement sequence applied in the pilot boreholes.

The bentonite was surprisingly resistant. The sampling tool could not be simply pushed with the drilling machine into the bentonite. The bentonite was very sticky and prevented a sliding of the sampling tool (see Figure 5). The sample tool had to be rotated while pushing. This resulted in a mechanical load and warm up of the samples, what restricted the desirable use of the sample material for extensive laboratory tests. It could be used only to a limited extent for analyses.

While the borehole wall was also affected by the drilling (warming up and stiffness) the geophysical borehole measurements could be performed properly, because both methods in principal are able to “look behind” the altered borehole wall zone (see Chap. 4 and 5).

At the end borehole 1 was closed with a packer and was sealed additionally with a resin near the concrete plug to prevent disturbances of the backfill until the controlled dismantling planned for winter 2012.

The second borehole (BEB-PB2) was assumed to be used for a hydro test in the backfill (see Chap. 6). Nagra with the contractor Solexperts was in charge of this experiment. BGR drilled the borehole and agreed with Solexperts modifications of the probe and the details of the emplacement. The drilling was as difficult as it was for the first borehole. The drilling process led to a stiffened borehole wall most likely caused by the temperature impact. After the trouble-free emplacement of the hydro test probe in the 4.1 m long borehole with a diameter of 86 mm it was expected that the bentonite converges in a reasonable time and closes the gap between the probe and the borehole wall. A close contact between the wall and the probe is a prerequisite for the functionality of the hydro test. Unfortunately, the bentonite did not converges and the gap was not closed, even after nearly one year. For more details see Chap. 6.

As a result of the described difficulties (amongst others clotted drilling barrels) the boreholes could not be drilled to the end as planned (8 m). Both drillings were stopped at a depth of 4.2 m. Important experiences were made with the drilling and simultaneous sampling work which should be taken into account for future comparable experiments.

3 Sampling and analysis

Sampling of bentonite specimen at several borehole depths was part of the drilling and geophysical measurement workflow in borehole BEB-PB1.

3.1 Applied technique

Bentonite samples were obtained by pushing a Dames and Moore sampler against the bentonite when introduced in the borehole. The sampling tool was provided by Golder. An adequate adapter for connecting the sampler with the drilling machine was necessary. A slight rotation was needed to extract the tool in some cases. The description of the sampling tool (Dames and Moore sampler) and the sample procedure is given by the following photographs in Figure 13 to Figure 18.

Figure 13: Ring sampler with thin wall prolongation

Figure 14: Sampler

Figure 16: Ring, container and identification label for samples

Figure 15: Packing procedure for samples (plastic bag, container and labels)

Figure 17: Transport box for samples (made in metal and with foam protection)

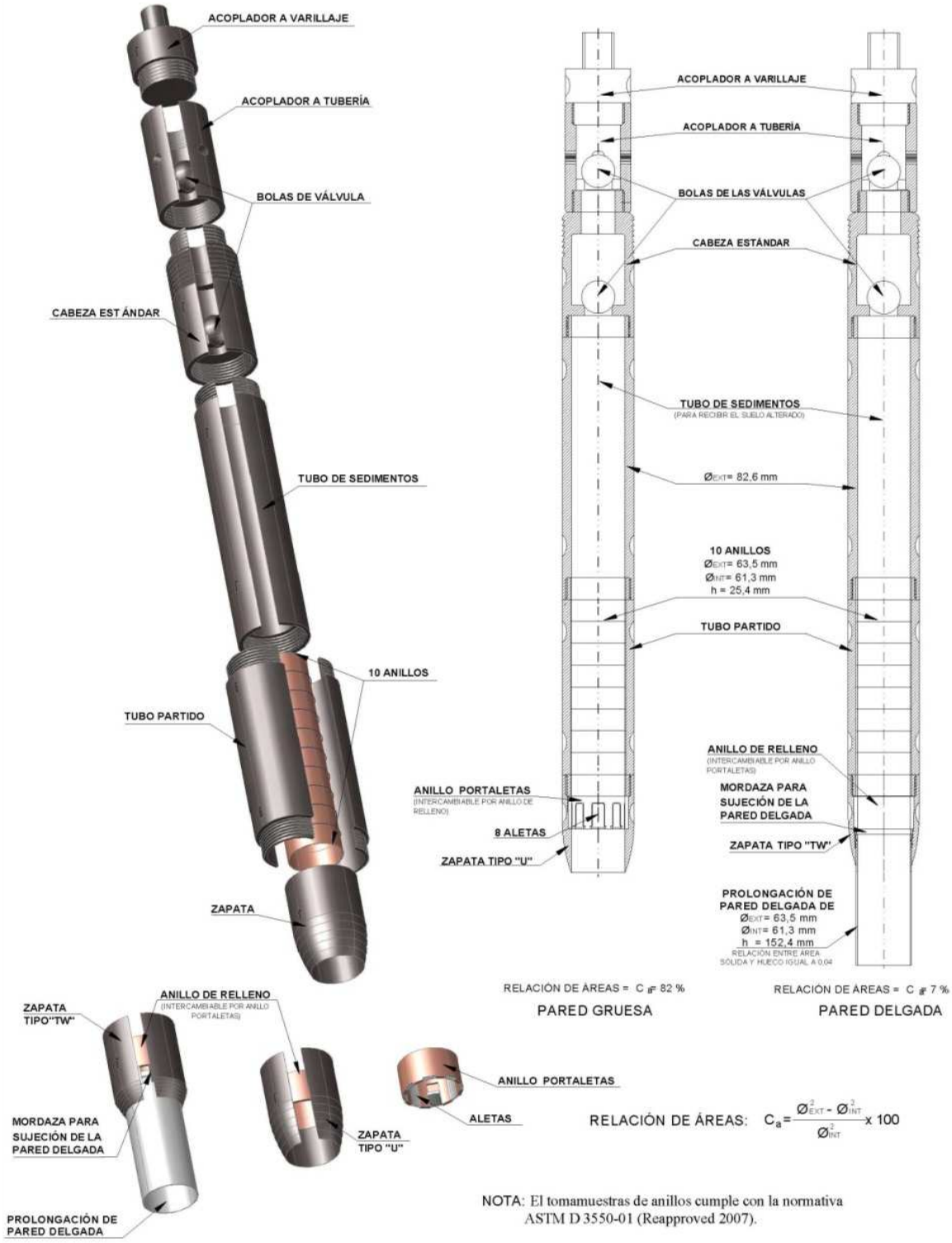

Figure 18: Layout and dimensions of the sampling tool

3.2 Results

The sampling tool was coupled to Craelius 50 drilling rods and pushed in and out using the drilling machine. The obtained samples were of 61.3 mm in diameter with a length up to 15 cm, thanks to the thin wall prolongation, and of 25 mm in length thanks to the rings housed in the sampler body. A total of 7 samples (see Table 3) were obtained and after being properly packed, they were sent to CIEMAT laboratories for analysis.

A detailed description on the analyses of samples gained from borehole BEB-PB1 is given in Villar and Gómez-Espina (2012). Some of the main results are compiled in the following Table 2. They should be taken with caution due to the suspected disturbance during the sampling.

Table 2: Results of the permeability tests in samples from borehole BEB-PB1 (Villar & Gómez-Espina, 2012)

Sample	Initial ρ_d (g/cm^3)	Final ρ_d (g/cm^3)	Initial w (%)	Initial S_r (%)	k_w (m/s)	Final w (%)	Final S_r (%)	T (°C)
M1		1.39	33.2	84	$3.7 \cdot 10^{-13}$	36.1	103	23
M2	1.42	1.27	33.0	99	$1.1 \cdot 10^{-12}$	42.7	103	19
M2-2	1.40	1.36	32.9	95	$3.1 \cdot 10^{-13}$	37.4	102	25
M-3	1.41	1.39	33.8	99	$3.1 \cdot 10^{-13}$	36.1	106	22
M-4	1.40	1.38	34.2	100	$4.3 \cdot 10^{-13}$	35.9	104	22
B-3	1.21	1.14	33.9	75	$9.3 \cdot 10^{-12}$	51.4	101	24

Table 3: Samples obtained from borehole BEB-PB1

Sample	Date of sampling	Borehole	Initial weight	Weight at reception (5/09/2011)	Sample depth	Comments
M1	23/08/2011 10:20 h	BEB-B1	719 g	718 g	2,20 m	Sample of 7 cm in length
M2	23/08/2011 11:17 h	BEB-B1	910 g	910 g	2,43 m	Sample of 9 cm in length
M3	23/08/2011 18:00 h	BEB-B1	1175 g	1174 g	3,20 m	See note*
M4	24/08/2011 12:15 h	BEB-B1	570 g	570 g	4,0 m	-
B1	23/08/2011 10:53 h	BEB-B1	164 g	164 g		Taken from the drilling tool. Looked homogeneous.
B2	23/08/2011 11:36 h	BEB-B1	120 g	120 g	2,52 m	-
B3	23/08/2011 16:05 h	BEB-B1	337 g	336 g	2,90 m	Taken from the drilling tool after more than 1.5 h. The sampler looked wet between 2.70 m and 3.20 m

MX: Unaltered sample

BX: Altered sample

* It is not sure this can be considered unaltered sample: the sampler was pushed in 16 cm but it was observed that it had only 12 cm of bentonite inside. However, as the thinwall sampler was recovered by drilling, it was found completely filled and the tool was quite warm.

4 Geoelectrical borehole measurements

High resolution geoelectrical borehole measurements were performed in borehole BEB-PB1 (B1) at several times during and after the drilling. The applied geophysical method aimed at the in-situ characterization of the consolidated bentonite material, especially to assess the level of homogenization with the help of geoelectrical resistivity data.

4.1 Fundamentals of DC Geoelectrics

To determine the spatial resistivity distribution (or its reciprocal – conductivity) in the ground, a direct current (DC) is introduced in the ground through two point electrodes (A,B).

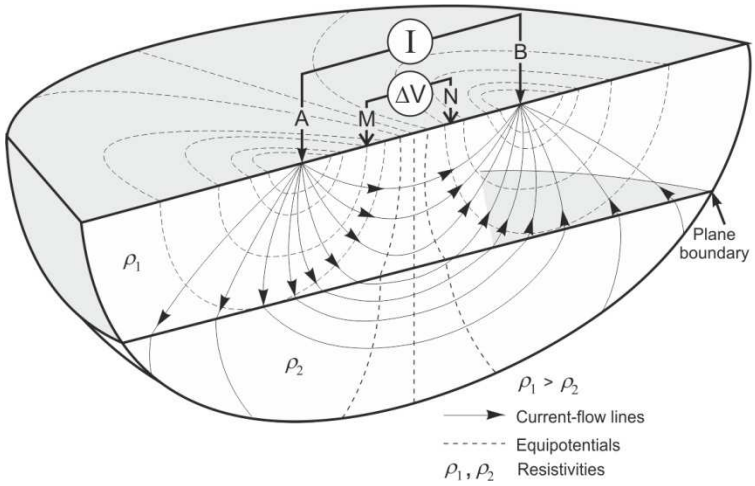

Figure 19: Principle of resistivity measurement with a four-electrode array (after Knödel et al., 2007)

The produced electrical field is measured using two other electrodes (M,N), as shown in Figure 19. A point electrode introducing an electrical current I will generate a potential V_r at a distance r from the source. In the case of a four-electrode array shown in Figure 16 consisting of two current electrodes (A,B) that introduce a current I and assuming a homogeneous half-space, the potential difference ΔV between the electrodes M and N can be calculate as follows:

$$\Delta V = \rho I \left[\frac{1}{2\pi} \left(\frac{1}{\overline{AM}} - \frac{1}{\overline{AN}} - \frac{1}{\overline{BM}} + \frac{1}{\overline{BN}} \right) \right]$$

$\overline{P_1P_2}$ denotes the distance between two points P_1 and P_2. Replacing the factor in square brackets by $1/K$, we obtain the resistivity of the homogeneous half space as follows:

$$\rho = K\frac{\Delta V}{I}$$

The parameter *K* is called configuration factor or geometric factor. For inhomogeneous conditions it gives the resistivity of an equivalent homogeneous half-space. For this value the term apparent resistivity ρ_a is introduced, which is normally assigned to the center of the electrode array. Multi-electrode resistivity meters enable the measurement of 2D resistivity surveys (2D imaging). The advantages of this kind of measurements are their high vertical and horizontal resolution along the profile. Figure 17 shows a commonly used setup of a Wenner-α configuration. All electrodes are placed equidistantly (distance *a*) along a profile. The configuration factor for this special configuration is given by $K = 2\pi a$. The diagram displaying the apparent resistivity as a function of location and electrode spacing is called pseudosection and provides an initial picture of the resistivity distribution. Other commonly used arrays are Schlumberger, dipole-dipole, Wenner-β (a special dipole-dipole configuration) or pole-dipole. The Wenner-α configuration is a good compromise between spatial resolution on the one hand and the signal-to-noise ratio on the other hand. In case of full-space conditions, the geometric factor is multiplied by a factor of 2.

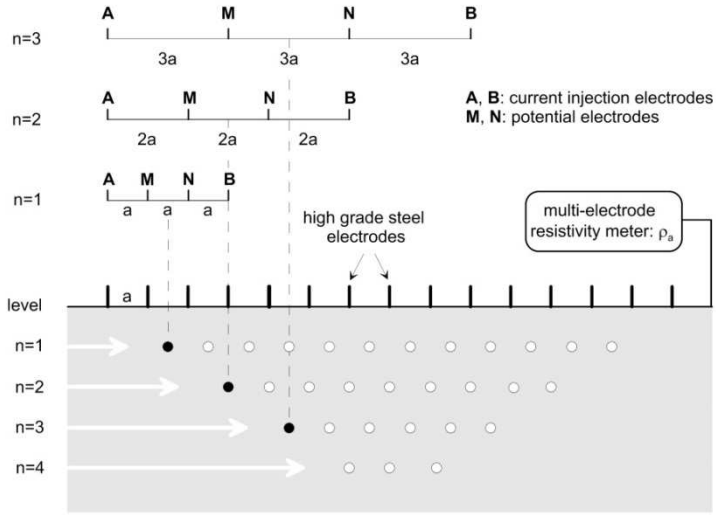

Figure 20: Setup for a 2D resistivity measurement (imaging) using a Wenner-α electrode configuration and presentation as a pseudosection (modified after Knödel et al., 2007)

4.2 Inversion

An inversion process of the measured data is necessary for the final interpretation. This process transforms the apparent resistivities into a reliable model discretized into a distinct number of elements of homogeneous resistivity. Mathematical an inversion algorithm minimizes iteratively the data functional defined by (see Günther et al., 2006)

$$\Phi_d(\mathbf{m}) = \left\|\mathbf{D}(\mathbf{d} - \mathbf{f}(\mathbf{m}))\right\|_2^2 - \lambda\left\|\mathbf{C}(\mathbf{m} - \mathbf{m}^0)\right\|_2^2$$

with

- the vector of logarithms of N single data $\mathbf{d} = \left(\log(\rho_1^a), \log(\rho_2^a), \ldots, \log(\rho_N^a)\right)^T$
- the vector of logarithms of M single model parameters $\mathbf{m} = \left(\log\rho_1, \log\rho_2, \ldots, \log\rho_M\right)^T$
- the model response $\mathbf{f}(\mathbf{m})$
- the vector of logarithms of M single start model parameters $\mathbf{m}^0 = \left(\log\rho_1^0, \log\rho_2^0, \ldots, \log\rho_M^0\right)^T$
- the weighting matrix $\mathbf{D} = \mathrm{diag}\left(1/\varepsilon_i\right)$ (ε_i is the associated error of the data point ρ_i^a)
- the constraint matrix $\mathbf{C}$
- the regularization parameter λ

The logarithms are used to ensure positivity of all resistivities. The forward operator is generally obtained by finite-difference (FD) or finite-element (FE) methods (Rücker et al., 2006). All inversions are performed using the non-commercial software BERT (Boundless Electrical Resistivity Tomography) developed by Th. Günther[1] and C. Rücker[2]. BERT allows the consideration of any geometry (2D, 3D, topography, bounded/unbounded, electrode shapes,…) and provides full control of the whole inversion process.

[1] Leibniz Institute of Applied Geophysics, Hannover

[2] Technical University of Berlin, Department of Applied Geophysics

4.3 Data

The borehole measurements were performed using a special borehole tool developed by BGR. Test measurements started 23/08/2014 afternoon. The main geoelectrical measurement was run in the afternoon 24/08/2014.

Figure 21: BGR borehole tool for resistivity measurements

The tool (see Figure 21) has a diameter of 80 mm and is designed for 86 mm boreholes. Greater diameters can be performed with special adapters. It contains 50 electrodes placed on 10 single modules which are pressed at the borehole wall by pneumatic cylinders. The electrodes are equally spaced with a distance of 15 mm. In the pilot borehole 3 single measurements are done in Wenner-α configuration (partly overlapping) in downward direction (180°).

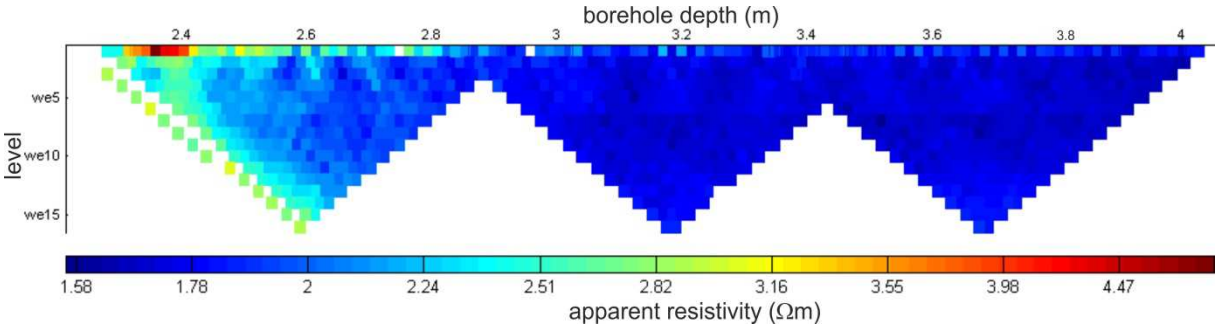

Figure 22: Pseudosection composed of 3 single Wenner –α measurements partly overlapping in the pilot borehole

Figure 22 shows the composed pseudosection, corrected with the configuration factors for borehole geometry. In the first part (until 2.4 m) higher apparent resistivities are visible, while at higher depths the apparent resistivities are quite low (< 2 Ωm).

4.4 Results

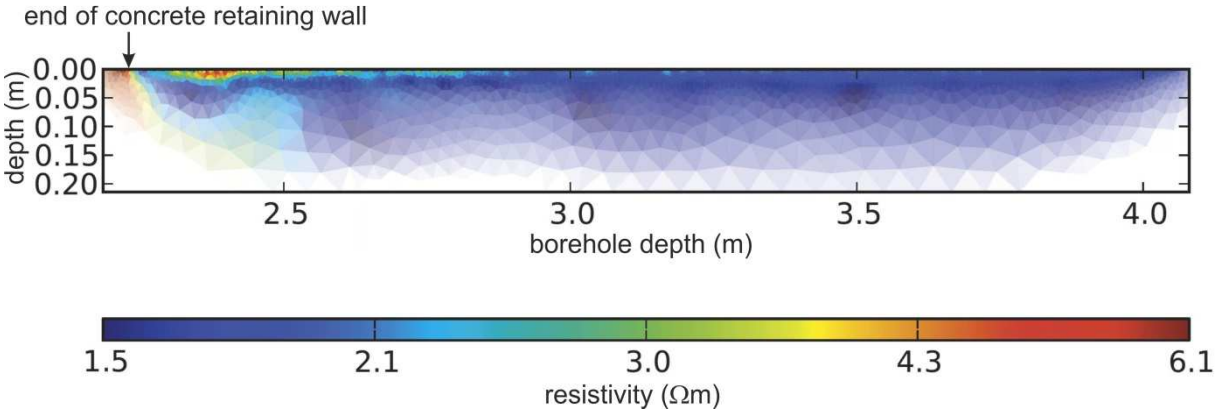

Figure 23: Inverted resistivity section of the pilot borehole, direction downwards (180°)

The inversion result is shown in Figure 23. The concrete retaining wall is marked clearly with higher resistivity (>20 Ωm) and range to a borehole depth of about 2.2 m. Up to 2.9 m borehole depth a small zone of higher resistivities are visible directly at the borehole wall. This can be interpreted as the borehole damaged zone, a result of the drilling process (heating, drying). Behind 3 m the medium looks very homogeneous. Figure 24 shows the inversion result for the second single measurement, but displayed with a smaller resistivity range. The borehole damaged zone is also clearly obvious and is ranging ~2 cm in the granular backfill bentonite material. The undisturbed material is characterized by resistivities below 2 Ωm.

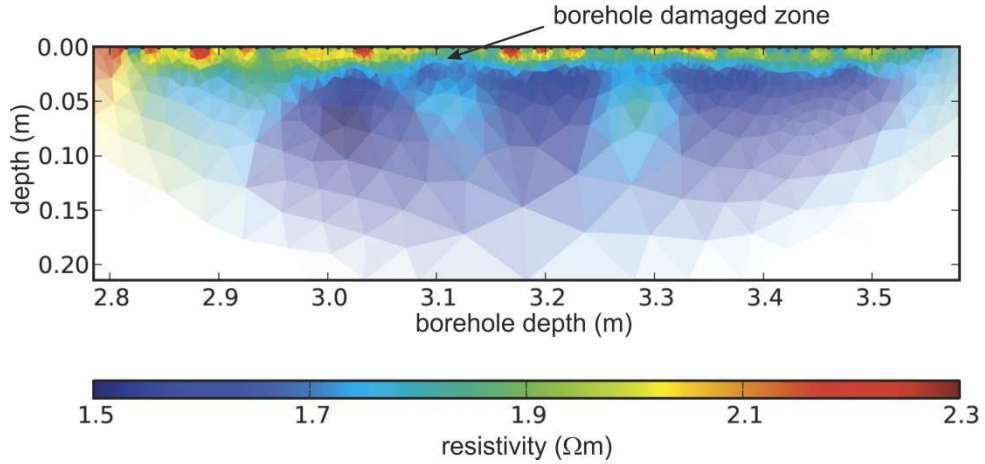

Figure 24: Inversion result of the second measurement. The borehole damaged zone can be detected ranging up to ~2 cm in the granular backfill bentonite material.

5 Ultrasonic borehole measurements

The ultrasonic borehole measurements which were applied in the same borehole BEB-PB1 where the geoelectrical measurements were performed aimed also at a high spatial resolution for the characterization of the consolidated bentonite. Furthermore, the measurements should provide information concerning the state of homogenization of the backfill material. Measurements were conducted in August 24, 2011 in the morning and repeated in the afternoon.

5.1 Measurement principle

Ultrasonic interval velocity measurements (IVM) were applied in the horizontal borehole BEB-PB1 with a sensor orientation of 0° (12 o'clock). This type of borehole measurement was used for the characterization of the rock in many underground facilities particularly in clay rock formations. The principal of this single borehole measurement method is shown in Figure 25 and described in more detail in Schuster et al. (2001) and Schuster (2012). The older mini sonic probe as shown in Figure 25c was used.

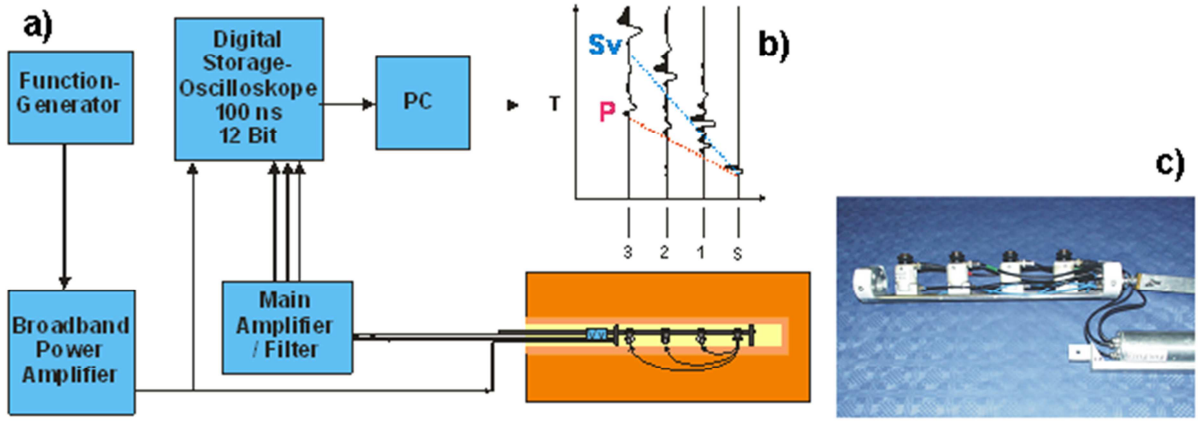

Figure 25: Principal of ultrasonic interval velocity measurements. a): Flow chart of the entire system. b): Derived seismic traces at one emitting point. c): BGR ultrasonic borehole probe.

The measurements started at 2.4 m (emitter position) in the consolidated bentonite, about 15 cm behind the concrete plug. Every 10 cm a measurement was performed with the result that every 10 cm a common shot point (CSP) data set was produced. Exemplarily such a CSP section is shown in Figure 25b with the marked first arrival phase (P-wave onset) and the vertically polarized S-wave onset (Sv). All CSP data sets are resorted to constant offset

data sets (COF) for an easier first arrival phase picking. Both data sets are shown as COF-sections in Figure 27 (morning measurement) and Figure 28 (afternoon measurement).

5.2 Data and processing

The interval velocity measurements were repeated after 5 hours with the same recording parameters and nearly at the same emitter and receiver locations. The first measurement was conducted only between 2.1 m (receiver R3) and 3.58 m (S1) and the second one between 2.1 m and 4.1 m. Because the borehole wall changed remarkable during this short period of time and this is an important observation we present all related data for a better and reliable assessment. From the COF-sections presented in Figures 27 and 28 the travel times of first arrival phases were distinguished. Only P-wave phases could be distinguished reliable and picked. For the shortest distance between emitter and receiver (R1, 10 cm) the reliability of picks is very good. For the R2 data it becomes weaker and for the 30 cm distance (R3) the quality is rather poor. As can be seen in the related COF-sections later parts of the phases are well developed. Because they are clearly related to the first arrival phases they were also picked in order to enhance the reliability of the first arrival picks. In Figure 26 an example of a seismic trace with excellent assignable arrival phases for a P- and S-wave onset (P0 and S0) is shown. Furthermore, several relevant characteristic signal phases are marked (PM, PM34, PM54, SM, SM34 and SM54) which are used in general for a standard processing.

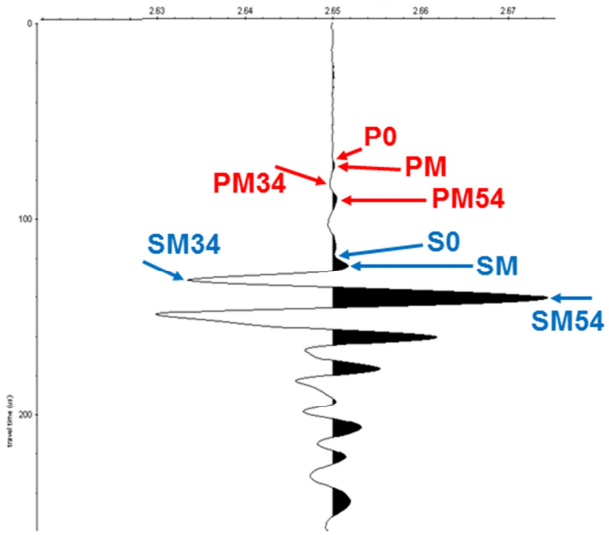

Figure 26: Seismic trace with different assigned phases

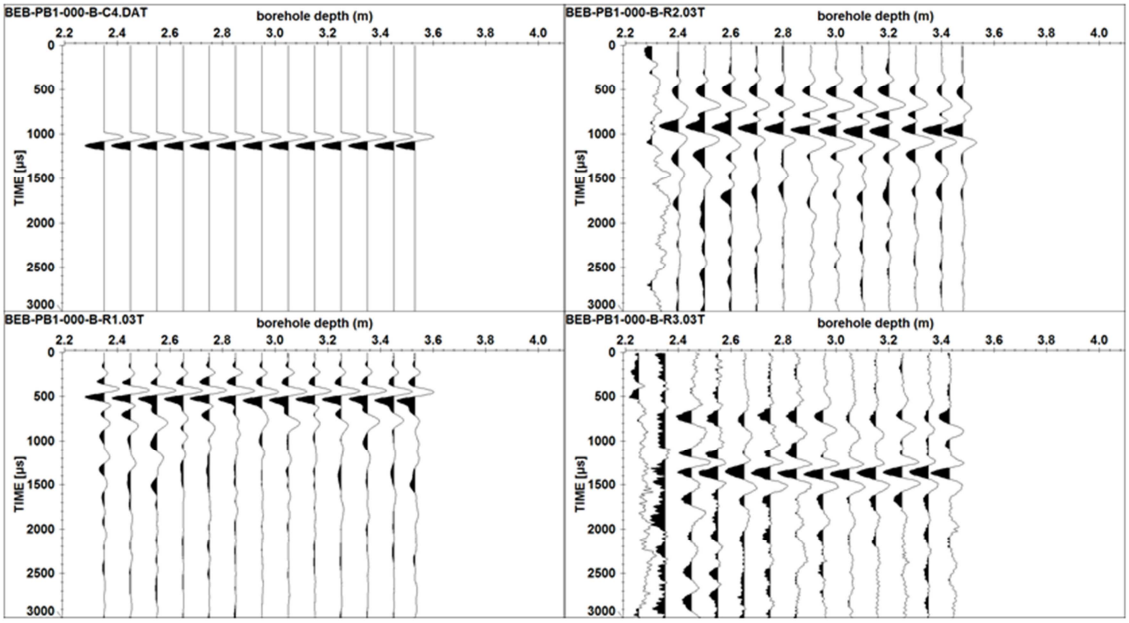

Figure 27: COF-sections of IVM data set B (morning measurement), trace normalized display. In the upper left plot the emitted signal is displayed, then in counter clockwise order: receiver R1, R3, R2.

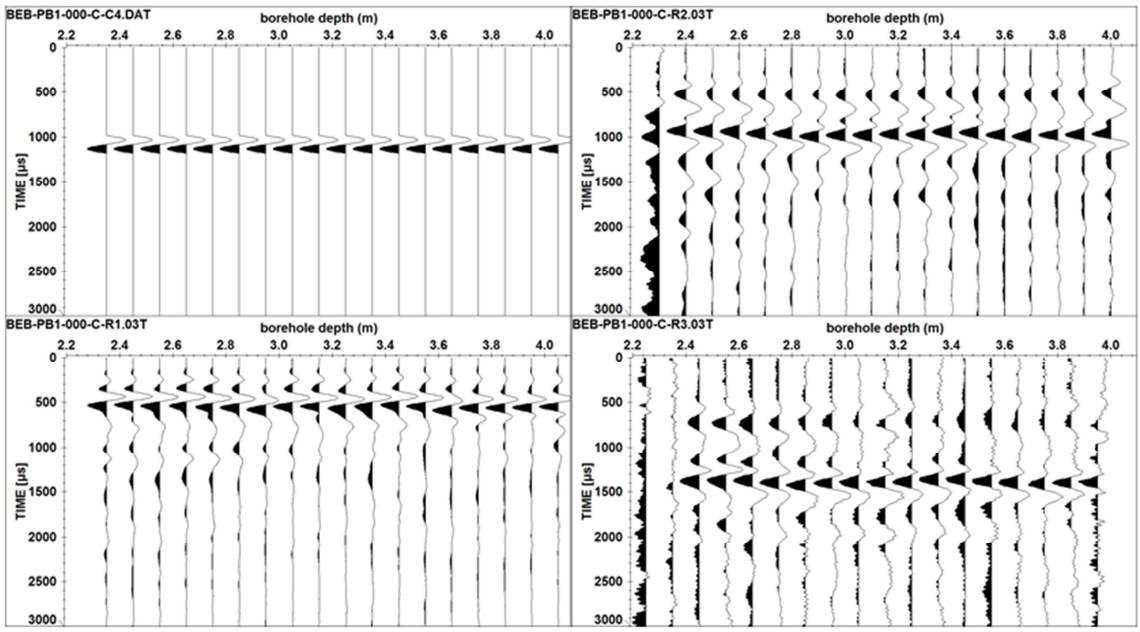

Figure 28: COF-sections of IVM data set C (afternoon measurement), trace normalized display. In the upper left plot the emitted signal is displayed, then in counter clockwise order: receiver R1, R3, R2.

In Figure 29 the different travel times related to the P-wave phase are presented for both measurements. They were used to get more confidence in the appropriate first arrival picks.

S-wave onsets are difficult to determine, because they interfere with reverberations from P-wave phases. They are not considered here.

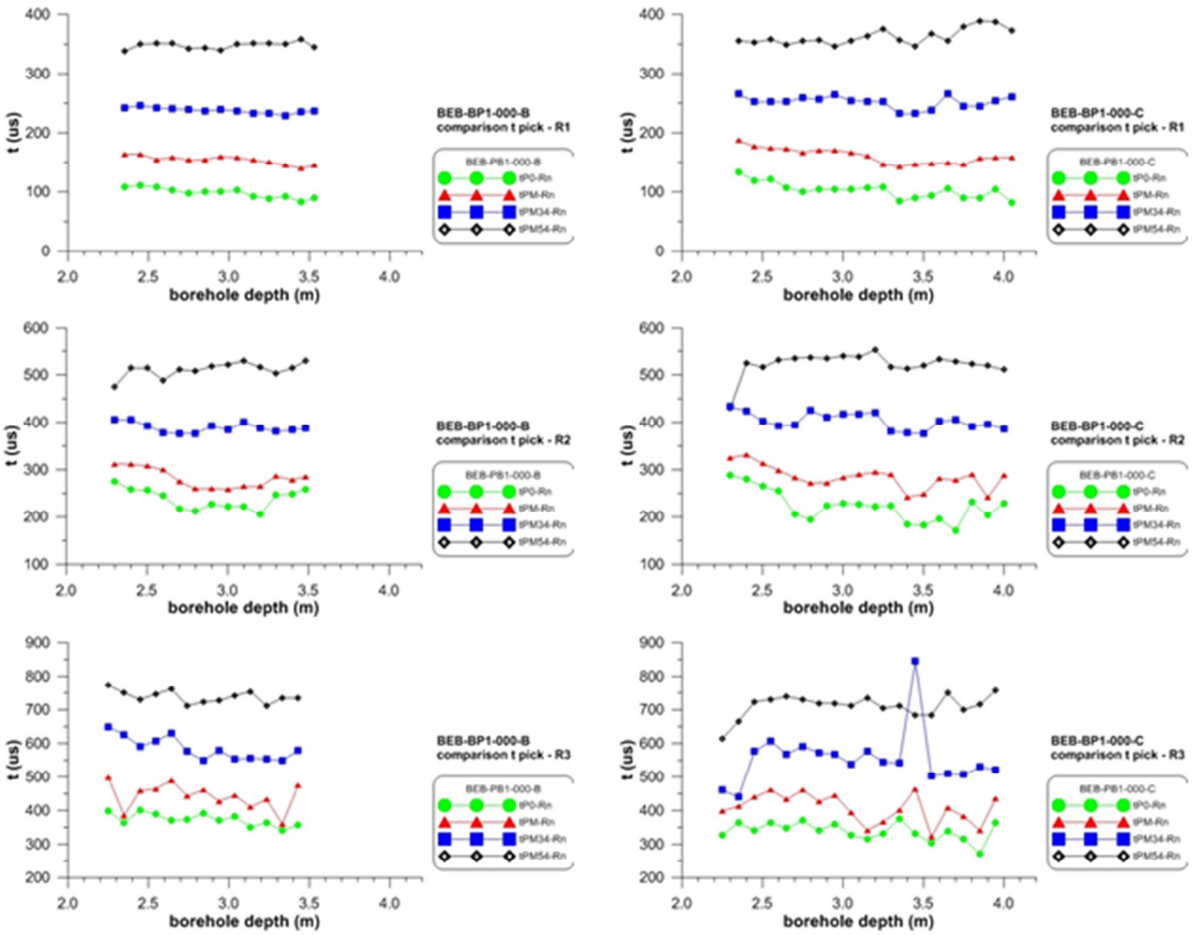

Figure 29: Comparison of picked P-wave travel times for different phases (tP0, tPM, tPM34, tPM54, cf. Fig.26).

With the help of the picked first arrival times the related apparent P-wave velocities $v_{p\text{-}Ri}$ for emitter - receiver R1 distance (10 cm), R2 (20 cm) and R3 (30 cm) were calculated via $v_p = L / t$, where L is the distance and t the travel time. At this stage the geometrical simplest travel path for the wave propagation is assumed (straight line). For a rock without any disturbance and no borehole wall disturbances this velocity is very close to the “real, undisturbed” velocity. In reality the travel paths are influenced by the v_p-gradients and disturbances around the borehole wall (Borehole disturbed Zone, BdZ). Schuster (2012) presented a method to determine and calculate the extent and degree of such BdZ features with the help of seismic parameters derived from IVM. The extent of the up to now investigated BdZ features ranges between several millimeters and several centimeters.

The apparent p-wave velocities $v_{p\text{-}Ri}$ and the BdZ corrected velocity $v_{p\text{-}cor}$, which give a more quantitative impression of the state of the material, are presented in Figure 30. For both measurements (morning and afternoon) and all receivers a lateral trend from lower to higher velocities is visible. In general for both data sets the $v_{p\text{-}R1}$ values are higher than the $v_{p\text{-}R2}$ values and the $v_{p\text{-}R2}$ values are higher than the $v_{p\text{-}R3}$ values. This points to an exceptional eggshell like structure of the borehole wall.

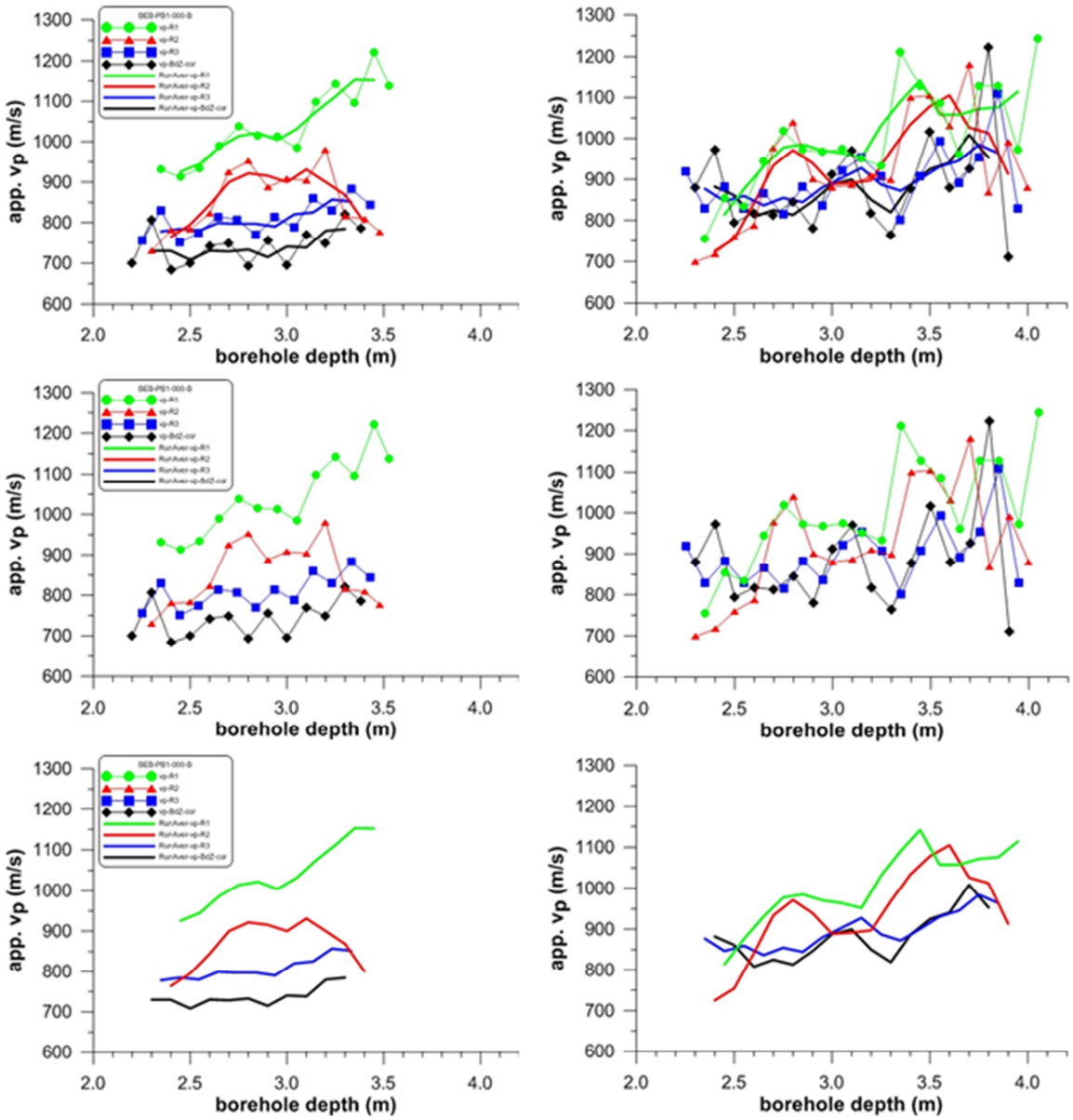

Figure 30: Derived P-wave velocities for different emitter – receiver distances (green: R1, red: R2, blue R3, black: BdZ corrected). Left: B data (morning). Right: C data (afternoon). Top: data with a running average over 3 points. Middle: Only individual data. Bottom: Only running average data over 3 points.

Furthermore, for the morning data the differences between the revivers are higher than for the afternoon data. This is a clear indication that the disturbed borehole wall changed within several hours towards more consolidation. According to our experiences made in clay rock the $v_{p\text{-}cor}$ derived from the afternoon data are close to the v_p expected behind the BdZ. From the EB experiment, where the first 576 days of the saturation of the bentonite were monitored with a seismic transmission experiment a v_p of 730 m/s was derived after 576 days (November 2013) of hydration (Schuster & Alheid, 2004B). Taking further eight years of saturation into account values between 800 m/s and 950 m/s (cf. Figure 30) seem to be reasonable.The differences in the velocities derived from the morning measurements are high ($v_{p\text{-}R1}$, $v_{p\text{-}R2}$, $v_{p\text{-}R3}$) and indicate that the extent of the BdZ is as high that the derived data are not sufficient for deriving the v_p behind the BdZ. A longer sonic probe would be necessary. In the Opalinus Clay at the Mont Terri Rock Laboratory a comparable repetition of ultrasonic measurements were performed. Within 20 hours the BdZ changed remarkable but both derived $v_{p\text{-}cor}$ were nearly identical (Schuster, 2012).

The data presented in Figures 27 and 28 as trace normalized wiggle plot sections are shown in Figures 31 and 32 as point mode plots and ensemble normalized. This type of display allows to assess the relative strength of the amplitudes along the borehole depth.

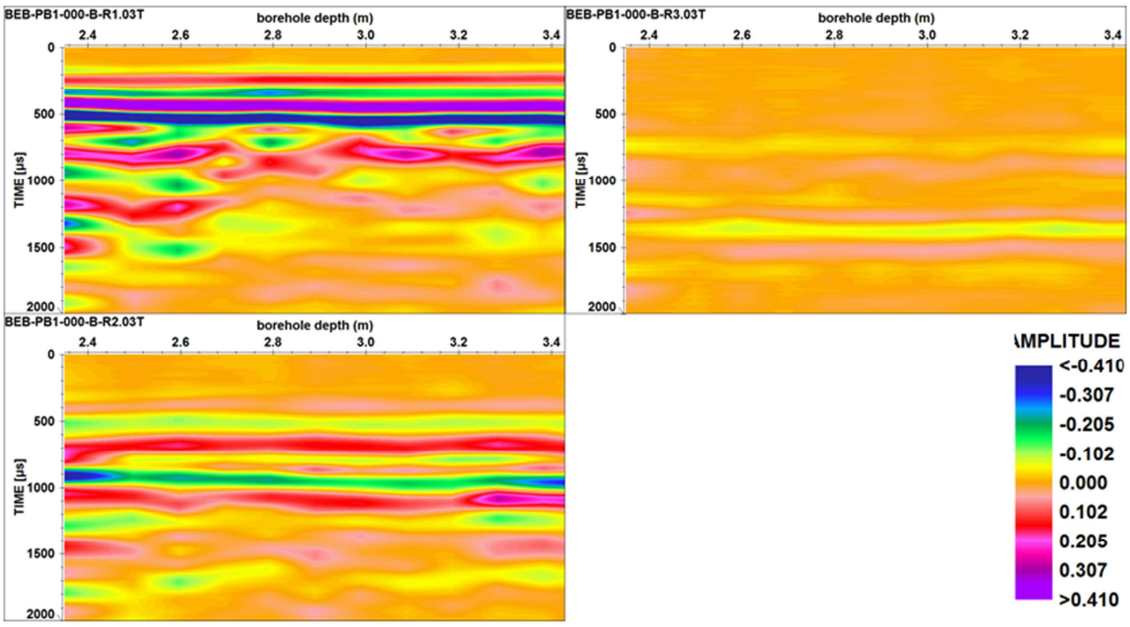

Figure 31: COF-sections of IVM data set B (morning measurement), ensemble normalized display, amplitudes are colour coded. In the upper left plot the receiver R1 signal is displayed, then in counter clockwise order: receiver R2, R3.

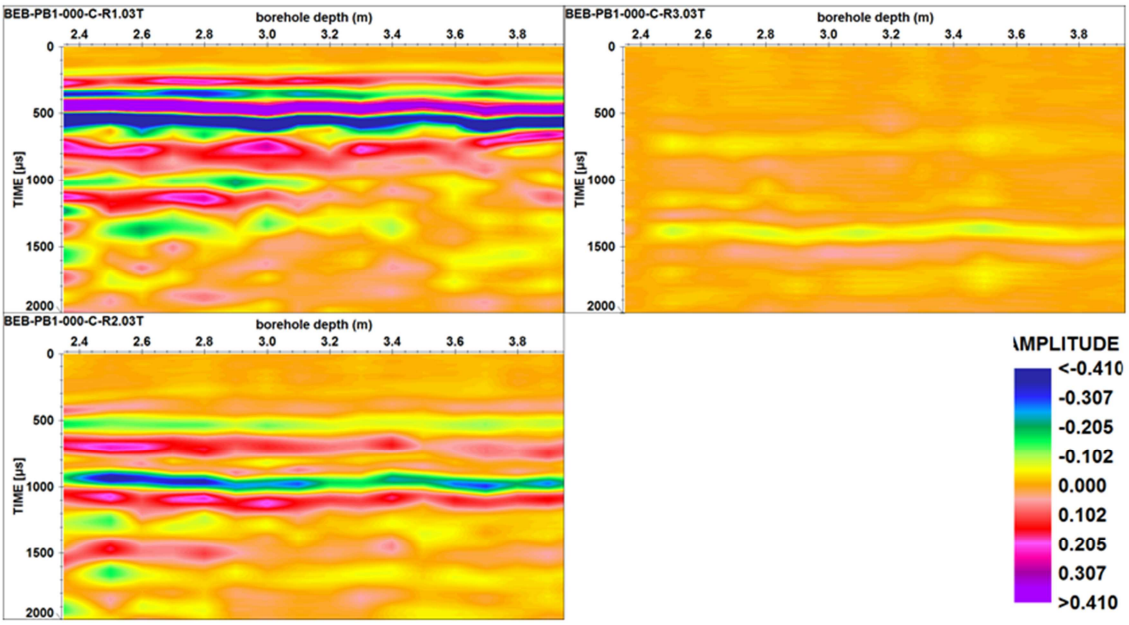

Figure 32: COF-sections of IVM data set C (afternoon measurement), ensemble normalized display, amplitudes are colour coded. In the upper left plot the receiver R1 signal is displayed, then in counter clockwise order: receiver R2, R3.

These plots show already qualitatively that along the borehole depth the amplitudes for the different emitter – receiver distances vary slightly. For later signal phases (greater travel times) the lateral variations appear more distinct.

In a more quantitative manner the amplitudes of seismic COF-sections can be taken into account for an assessment of the lateral variation of the bentonite along the borehole depth. For this reason the arithmetic mean of the sum of all samples for each single seismic trace was calculated. In Figure 33 the results are plotted for both measurements and for each emitter – receiver distance. For the three emitter - receiver distances (R1-10 cm, R2-20 cm, R3-30 cm) the differences, e. g. for one depth location, they are mainly related to the different length of travel paths. To assess the variation along the borehole only data from one receiver should be compared. The amplitude data are related to the damping behavior of the material. Because the emitter signal is well defined and was held constant and the coupling of the emitter and receiver piezos is controlled and general very good in a first attempt lower values (higher attenuation) imply a looser material and vice versa, higher values imply a more compacted/consolidated material. The lateral variations of the R3 data for the morning and afternoon measurement as well as along the borehole in both cases are in the same range. For the R1 and R2 data the lateral variations are more pronounced, what imply that changes in the borehole wall were going on.

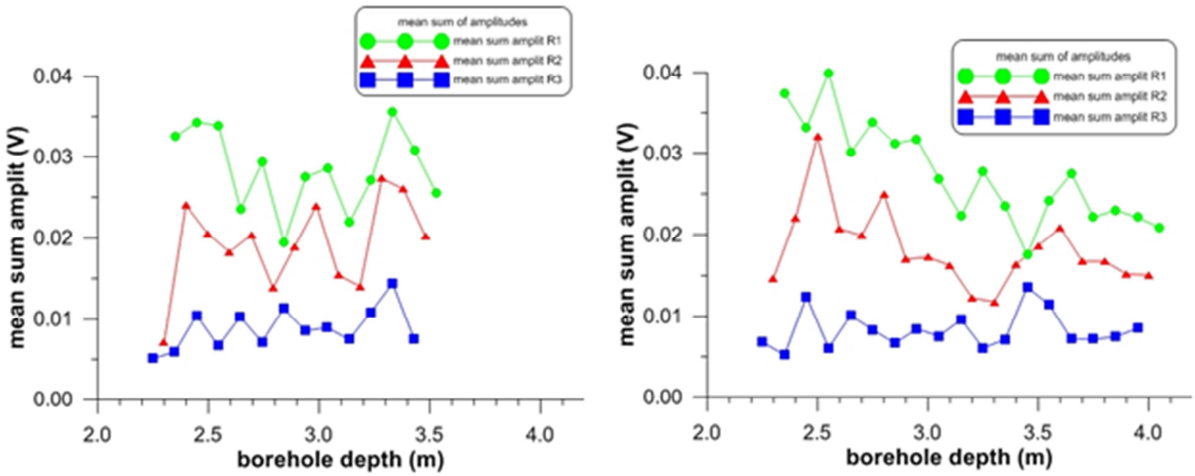

Figure 33: Arithmetic mean of the sum of amplitudes for different emitter – receiver distances (green: R1, red: R2, blue R3). Left: B data (morning). Right: C data (afternoon).

5.3 Results

All derived parameters show remarkable differences between the morning and afternoon data, which implies noticeable changes in the borehole wall.

All in all the bentonite appears homogeneous with a slight lateral trend towards greater borehole depth (afternoon measurements: slight $v_{p\text{-}cor}$ increase).

Remarkable changes in the BdZ between the morning and afternoon measurement but also for each measurement along the borehole wall were detected.

The derived BdZ corrected velocities seem to be reasonable when comparing it with seismic transmission data measured eight years before during the initial phase of the consolidation of the bentonite.

6 Hydro test

It was planned to conduct a hydro test in the borehole in order to estimate the hydraulic conductivity of the emplaced granular bentonite in-situ. This would have allowed comparing the in-situ measurements with the measurements conducted in the laboratory after dismantling the test.

Already from the start of the experiment it was well known that hydro testing in bentonite is not trivial and that there was a certain risk that the test could not be conducted properly.

6.1 Measurement principle

The hydraulic test interval section was located in axial tunnel direction at a distance of about 3 m from the concrete plug and in radial tunnel direction at a central position between the canister dummy (centre) and the host rock interface.

A casing was installed to avoid the borehole collapse and a packer system inside the casing was foreseen. The casing had a filter section of about 30 cm at the interval position. The casing filter size was adjusted so that the bentonite particles would not clog the filter. The filter section was installed in a distance between 3.26 m and 3.46 m from the plug wall which corresponds to a bentonite depth of about 1.04 m to 1.24 m. The casing wall thickness was designed to withstand about 20 bar total pressure. In addition, the casing duct through the concrete plug was sealed with resin.

The borehole instrumentation consisted of an inflatable double packer system installed inside the casing. Packer 1 seals the open end casing part and packer 2 towards the outer boundary. The measurement interval between both packers is equipped with two ports, one for pressure monitoring and one as flow line. The packer system required a minimum inner diameter of the casing of about 82 mm. A schematic drawing of the double packer system is shown in Figure 34 (the casing is not shown).

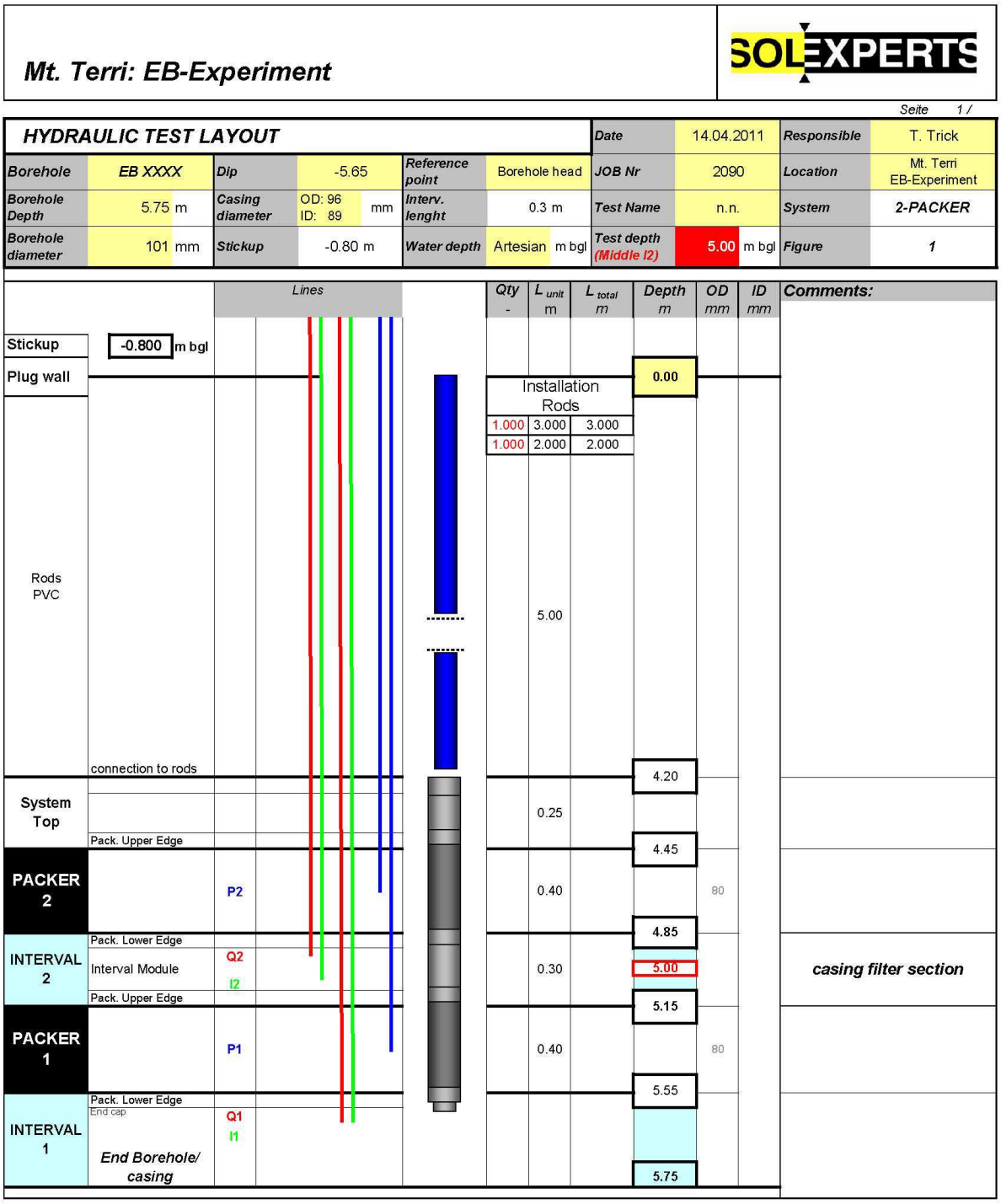

Figure 34: Schematic layout of the double packer system installed within the casing

It was planned to measure the hydraulic conductivity with a long-term hydraulic constant head injection test (HI-test). This could only be conducted after the gap between the casing and the granular bentonite had disappeared due to additional swelling of the bentonite after drilling. A pressure build up period should have started after the installation of the packer system and the interval saturation. Subsequently a HI test should have started by injecting

water (using synthetic Pearson's water) into the test interval. The HI flow phase should have been shut-in after one month and the following recovery phase should have been measured for about 6 weeks. The surface equipment, shown in Figure 35, consists of pressurization unit (pressure vessel) and flow rate measurement unit. The flow rate measurement unit comprises at least two flow meters to capture the different flow rate ranges.

A high flow range flow meter (Q1) was planned to be installed only during the initial flow phase (first day of injection) and a second (third) flow meter was planned to be installed to measure the mid to late test time flow rates. The interval pressure signal and the two or three flow meters output signals were planned to be connected to the Aitemin DAS where a few spare channels were available.

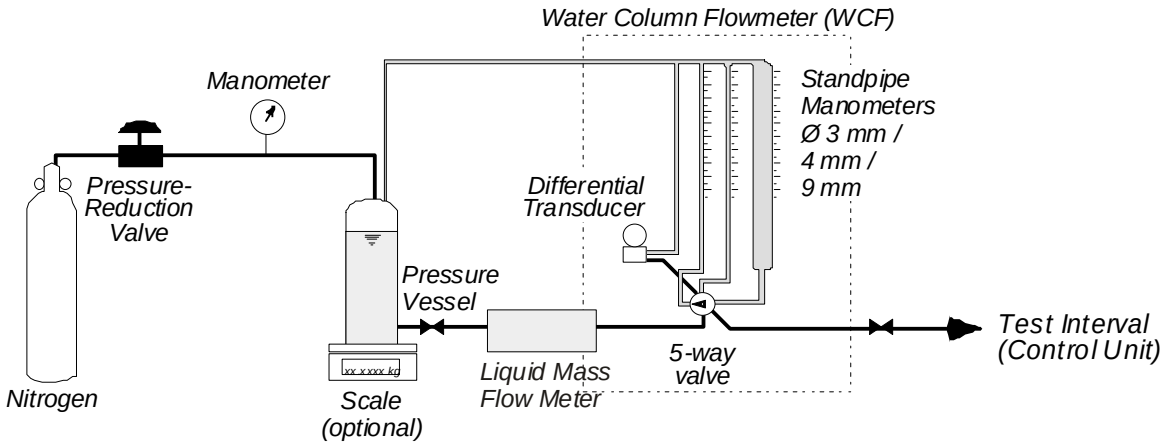

Figure 35: General hydraulic constant head injection test setup planned for the EB borehole.

The double packer would have been retrieved after the completion of the hydraulic test and a mechanical single packer installed to seal the casing at the casing filter section. A dummy at the rear end side should have avoided the bentonite from moving into the casing.

6.2 Data

The double packer was installed on 26 August 2011 and inflated to a 30 bar pressure. A vacuum test was conducted in the test interval. The vacuum was not sustained and the pressure increased within a few minutes to atmospheric.

This was attributed to the following

- The resin might not have been hard and the sealing not in place.
- The existing gap of 3 mm between casing and bentonite borehole wall was still open (no bentonite swelling took place in a sufficient manner).

In regular intervals, 4-6 weeks, the vacuum test was repeated to assess if the gap between the casing and the bentonite closed and it would be possible to conduct the hydro test. This was not the case, and until the moment the dismantling of the EB had to take place the vacuum could not be sustained, making hydro testing to be of no value.

6.3 Results

As the permeability of the granular bentonite was extremely low, the granular bentonite did not provide sufficient water to allow closing the gap between the casing and the bentonite through swelling. Therefore the hydro testing had to be abandoned as the casing could no longer be removed either. While this was a known risk for the test, it was possibly aggravated by the fact that the drilling technique that was selected caused some drying out of the bentonite close to the borehole wall. This was confirmed when analyzing the samples. Because of this even less water was available to induce swelling of the bentonite and close the gap.

It was concluded that hydro testing in bentonite should be re-evaluated to check under which conditions it would be feasible.

7 Accompanying geotechnical monitoring

A monitoring of several geotechnical key parameters was included in the EB Experiment. This was not part of the actual discussed task. Some data from these measurements are presented in Figure 36. They were extracted from the appropriate Aitemin data base and compiled by Aitemin. The evolution of total pressure data from eight locations in the EB niche are shown covering the time August 19, 2011 to August 29, 2011. The sensors are at a distance of 2.1 m from the concrete plug interface, what corresponds to 4.3 m for the here discussed geophysical profiles.

The response of the total pressure signals as a result of the drilling and sampling activities can be seen very clear. At several steps of the on-site activities the pressure values increase and / or decrease.

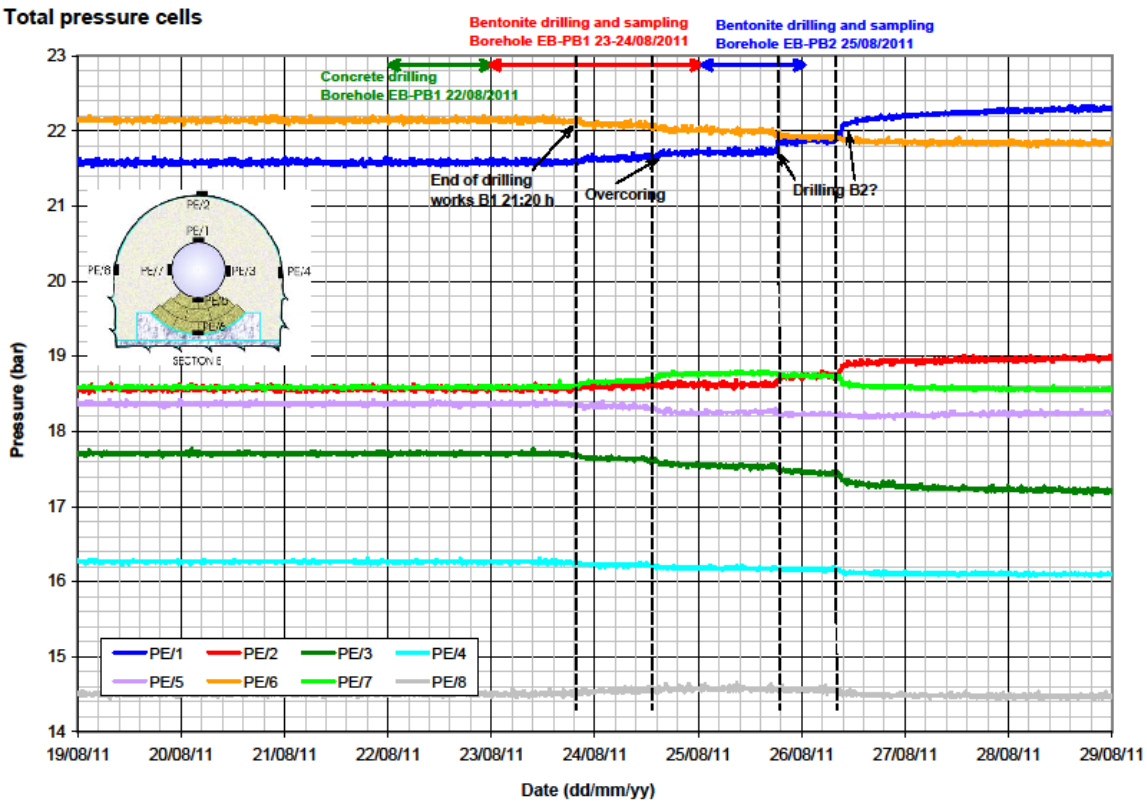

Figure 36: Evolution of total pressure data covering the relevant time of the pilot borehole activities.

8 Overall results and conclusions

The expected rapid convergence of the boreholes after the drilling did not occur, both boreholes stayed rather stable concerning the diameter. On the other hand the borehole wall in BEB-PB1 changed remarkably according to the derived geophysical parameters.

Both geophysical borehole methods showed that the bentonite, which was emplaced ten years before and hydrated artificially, seemed to be homogenized in the inspected area with some slight lateral changes.

Although the geoelectrical and the ultrasonic measurements were performed with different orientations of sensors (180° and 0°) a similar characteristic could be seen. Only slight lateral variations but a pronounced BdZ were derived.

The derived geophysical parameters are in good accordance with results gained in the initial phase of the EB Experiment and before and during the dismantling process.

9 Acknowledgements

The research leading to these results has received funding from the European Atomic Energy Community's Seventh Framework Programme (FP7/2007-2011) under grant agreement n° 249681.

The BGR contribution is co-funded by the German Ministry of Economy and Technology (BMWi), FKZ 02 E 10689.

We thank Thierry Theurillat (swisstopo) for his technical support of the on-site work.

10 References

Aitemin (2001): Engineered Barrier Emplacement Experiment in Opalinus Clay “EB” Experiment. TEST PLAN. Madrid, 76 pp.

Aitemin (2007): Engineered Barrier Emplacement Experiment in Opalinus Clay “EB” Experiment. Sensors data report Nº 19 and Mont Terri TN2007-11. Period 22/11/2001 to 30/06/2007, 38 pp.

Aitemin (2011): Engineered Barrier Emplacement Experiment in Opalinus Clay “EB” Experiment. TEST PLAN for Drilling of the GBM boreholes. Madrid 22 pp.

Furche, M. & Schuster, K. (2014): Engineered Barrier Emplacement Experiment in Opalinus Clay “EB” Experiment. Geoelectrical monitoring of dismantling operation. PEBS Deliverable D2.1-9.

Günther, T., Rücker, C. & Spitzer, K. (2006): Three-dimensional modeling and inversion of dc resistivity data incorporating topography – II. Inversion. – Geophys. J. Int. **166**: 506–517.

Knödel, K., Lange, G. & Voigt, H.-J. (2007): Environmental Geology – Handbook of Field Methods and Case Studies: 1357 S., 501 Abb., 204 Tab.; Berlin (Springer) – ISBN 978-3-540-74669-0

Palacios, B., Rey, M., Garcia-Siñerez, J. L., Villar, M. V., Mayor, C & Velasco, M. (2013): Engineered Barrier Emplacement Experiment in Opalinus Clay “EB” Experiment. As-built of dismantling operation. PEBS Deliverable D2.1-4

Rücker, C., Günther, T. & Spitzer, K. (2006): Three-dimensional modelling and inversion of dc resistivity data incorporating topography – I. Modelling. – Geophys. J. Int. **166**: 495–505.

Schuster, K., Alheid, H.-J. & Böddener, D. (2001): Seismic investigation of the Excavation damaged zone in Opalinus Clay, Engng. Geol. 61: 189-197.

Schuster, K. & Alheid H.-J. (2004A): EB: Engineered Barrier Experiment; Seismic Long Term Observation in the EB Niche, Mont Terri Technical Report TR 04-02, swisstopo, Wabern, Switzerland.

Schuster, K., Alheid, H.-J., Kruschwitz, S., Siebrands, S., Yaramanci, U., Trick, T., Manthei, G. (2004B), Observation of an Engineered Barrier Experiment in the Opalinus Clay of the Mont Terri Rock Laboratory (CH) with Geophysical and Hydraulic Methods, 2 posters and abstract, Euradwaste'04, Radioactive waste management - Community policy and research initiatives, Sixth European Commission Conference on the Management and Disposal of Radiactive Waste, 29. March - 1. April 2004, Luxembourg.

Schuster, K. (2012): Detection of borehole disturbed zones and small scale rock heterogeneities with geophysical methods, Proceedings of the EC-TIMODAZ-THERESA International Conference, Impact of thermo-hydro-mechanical chemical (THMC) processes on the safety of underground radioactive waste repositories, Luxembourg, 29 Sep. - 1 Oct. 2009, p. 135-145

Schuster, K. (2014): Engineered Barrier Emplacement Experiment in Opalinus Clay “EB” Experiment. Seismic Long-term Monitoring of EDZ Evolution. PEBS Deliverable D2.1-6.

Villar, M. V. & Gómez-Espina, R (2012): Permeability tests in samples from the EB experiment at Mont Terri (borehole EB-B1), Technical Note CIEMAT/DMA/2G210/06/12

Yaramanci, U. & Siebrands, S. (2003): Geoelectrical Characterization of the Disturbed Rock Zone in the Underground Rock Laboratory “Mont Terri”, TU Berlin, Department of Applied Geophysics, Internal report